

pletely by subsequent storms, or (iii) the dark deposits are so young that they have so far escaped burial. The first possibility is unlikely because the darkest patch measured on an image taken early in the Viking mission became obscured by a light blanket during the subsequent dust storms of 1977.

The second possibility will be explored in more detail. How fast does light-colored dust obscure dark materials? Thomas *et al.* (13) calculated that a coating of light-colored dust covering as little as 30 to 50% of a region would result in maximum contrast between light and dark areas on Mars. Such a coating could come from only one-quarter of the annual dust fallout distributed evenly over the Martian surface (17). The time needed for dust to completely bury a dark-patch deposit (22) having an assumed grain size of 10  $\mu\text{m}$  (an upper limit according to thermal-inertia measurements) would range from 30 years for densely packed dust to 1500 years for porous material; density of the latter corresponds to that of fine weathered glass (23). If dust fallout were erratic, the patches would be buried in 30,000 to 1,500,000 years (22). It appears that the dark patches would be buried rapidly and, if dust were never removed, they would be very young indeed.

However, removal of light-colored coatings is to be expected. How much would be removed during subsequent storms is difficult to assess. Some dust would certainly remain trapped in cracks and crevices and would eventually tend to lighten the dark patches. Thomas (10), considering the age of low-albedo splotches inside craters, suggested that the material had to be reworked continuously by saltation to prevent a rise in albedo due to a dust cover. For the thin dark streaks emanating from dark-crater splotches, Thomas (10) estimated a lifetime only of about 10 to 100 years because of the tenuous nature of the streaks and their susceptibility to wind action. The delicate structure of the feathery edges of the vent deposits in Valles Marineris would be blanketed or destroyed by mechanisms similar to those affecting the dark streaks from crater splotches. Thus, the third possibility is indicated: the dark patches are very young. In fact, they may be no older than a few million years at most.

It appears that the Valles Marineris tectonic troughs experienced a phase of mafic or ultramafic, pyroclastic volcanism. This observation is the first suggestion that Valles Marineris tectonism was accompanied by volcanism, as is common in most terrestrial rift systems. If this volcanism is indeed as young as it seems, Mars has been an active planet throughout most of its history.

#### REFERENCES AND NOTES

1. M. H. Carr, *J. Geophys. Res.* **79**, 3943 (1977).
2. D. H. Scott, *ibid.* **87**, 9839 (1982).
3. G. G. Schaber, K. C. Horstman, A. L. Dial, *Proc. Lunar Planet. Sci. Conf.* **9**, 3433 (1978).
4. H. Frey, B. L. Lowry, A. C. Scott, *J. Geophys. Res.* **84**, 8075 (1979).
5. P. W. Francis and C. A. Wood, *ibid.* **87**, 9881 (1982).
6. C. Pieters, T. B. McCord, Stanley Zisk, J. B. Adams, *ibid.* **78**, 5867 (1973).
7. G. H. Heiken, D. S. McKay, R. W. Brown, *Geochim. Cosmochim. Acta* **38**, 1703 (1978).
8. G. H. Heiken and D. S. McKay, *ibid.*, p. 1703.
9. B. R. Hawke *et al.*, *Proc. Lunar Planet. Sci. Conf.* **10**, 2995 (1979).
10. P. Thomas, *Icarus* **57**, 205 (1984).
11. Orbits 912 through 917 (resolution about 60 m per pixel) and 815 (resolution 25 to 30 m per pixel).
12. H. A. Pohn and R. L. Wildey, *U.S. Geol. Surv. Pap.* **599-E** (1970).
13. P. Thomas, J. Veverka, D. Gineris, L. Wong, *Icarus* **60**, 161 (1984).
14. R. B. Singer, E. Cloutis, T. L. Roush, P. J. Mouginis-Mark, B. R. Hawke, *Lunar Planet. Sci.* **15**, 794 (1984).
15. T. B. McCord *et al.*, *J. Geophys. Res.* **87**, 10129 (1982).
16. P. R. Christensen, *Icarus* **56**, 496 (1983).
17. \_\_\_\_\_ and H. H. Kieffer, *J. Geophys. Res.* **84**, 8233 (1979).
18. A. R. Peterfreund, *Icarus* **45**, 447 (1981).
19. R. Greeley, R. Leach, B. White, J. Iversen, J. Pollack, *Geophys. Res. Lett.* **7**, 121 (1980).
20. D. S. McKay, G. H. Heiken, G. Waits, *Proc. Lunar Planet. Sci. Conf.* **9**, 1913 (1978).
21. B. K. Lucchitta, *J. Geophys. Res.* **84**, 8097 (1979).
22. The calculation assumes one-half the annual dust loading of the atmosphere [annual loading,  $4 \times 10^3$  g/cm<sup>2</sup> per year; see J. B. Pollack, D. S. Colburn, M. Flasar, R. Kahn, C. E. Carlston, D. Pidek, *J. Geophys. Res.* **84**, 2929 (1979)] and a density of individual dust grains of 3 g/cm<sup>3</sup>. This results in a 7- $\mu\text{m}$  annual layer of densely packed light dust each year, and a 330- $\mu\text{m}$  annual layer of porous dust (1/50 of solid material) [E. N. Wells, J. Veverka, P. Thomas, *Icarus* **58**, 331 (1984)]. For erratic dust fallout 1/1000 the annual fallout was considered.
23. R. B. Singer, *J. Geophys. Res.* **87**, 10159 (1982).
24. Supported by NASA's Planetary Geology and Geophysics Program.

8 August 1986; accepted 26 November 1986

## Superconductivity at 52.5 K in the Lanthanum-Barium-Copper-Oxide System

C. W. CHU,\* P. H. HOR, R. L. MENG, L. GAO, Z. J. HUANG

A superconducting transition with an onset temperature of 52.5 K has been observed under hydrostatic pressure in compounds with nominal compositions given by  $(\text{La}_{0.9}\text{Ba}_{0.1})_2\text{CuO}_{4-y}$ . Possible causes for the high-temperature superconductivity are discussed.

THE SEARCH FOR HIGH-TEMPERATURE superconductivity and novel non-phonon-mediated superconducting mechanisms is one of the most challenging tasks of condensed matter physics and material science. As a consequence, many compounds have been tested and numerous mechanisms proposed during the last three decades. However, only recently has a superconducting transition temperature ( $T_c$ ) of 35 K been reported (1), and later of 40.2 K under hydrostatic pressure (2), almost twice the value of 23.2 K first reported (3) in  $\text{Nb}_3\text{Ge}$  sputtered thin films. Although the suggestions (4) of spin fluctuation-assisted electron-pairing and triplet superconducting states in heavy fermion superconductors are consistent with some experimental data, unambiguous evidence has yet to be established. No definitive guidelines exist, to date, for predicting those material systems that will exhibit high  $T_c$  or novel superconducting mechanisms. In this respect, an empirical search for new materials remains the most effective approach. It has been suggested (5) that it may be fruitful to investigate superconductivity under various conditions (high pressure, for example) in compounds generally not favorable for superconductivity. The superconducting oxide systems are examples of such systems.

Oxidation is known to degrade the metallic and, in particular, the superconducting characteristics of matter. However, superconductivity has been observed in some highly oxidized perovskites and related compounds (6) such as  $\text{SrTiO}_{3-x}$ ,  $\text{Na}_x\text{WO}_3$ ,  $\text{Li}_{1+x}\text{Ti}_{2-x}\text{O}_4$ , and  $\text{BaPb}_{1-x}\text{Bi}_x\text{O}_3$ , with a  $T_c$  reaching 13 K for the last two oxides. Such a high  $T_c$  is especially unusual for  $\text{BaPb}_{1-x}\text{Bi}_x\text{O}_3$ , which has no  $d$ -electrons near the Fermi level and exhibits an extremely low electron density of states. In spite of the great variation of their  $T_c$  values these oxides have several similarities (7). For instance, superconductivity occurs only over a narrow range of  $x$  values, with the highest  $T_c$  near the metal-insulator phase boundary. All these oxides possess oxygen octahedrons and mixed valence (that is, tungsten, titanium, bismuth, and copper) sites. Near the metal-insulator phase boundary, soft modes or interfaces (due to concentration fluctuations) may exist. Oxygen octahedrons in proper arrangements are known to be closely associated with soft ferroelectric modes. Mixed valence systems have been considered

Department of Physics and Space Vacuum Epitaxy Center, University of Houston, Houston, TX 77004.

\*Also at the Division of Materials Research, National Science Foundation, Washington, DC 20550.

favorable for polaron formation. Soft modes (8), interfaces (9), and polarons (10) have been suggested to provide avenues for enhanced electron-pairing interactions, either conventional or nonconventional, leading to a higher  $T_c$ . A new system, La-Ba-Cu-O (lanthanum - barium - copper - oxide, or LBCO), has just been added to this oxide family by Bednorz and Müller (1).

Recently, Bednorz and Müller (1) have examined the electrical properties of the  $\text{La}_{1-x}\text{Ba}_x\text{CuO}_{3-y}$  compound system. On cooling, the resistance  $R$  of samples with  $x \leq 0.2$  initially decreased and then increased prior to a sharp resistance drop, with the drop starting at temperatures as high as  $\sim 35$  K. For some samples, a zero- $R$  state was achieved below  $\sim 12$  K, although all samples contained multiple phases. The  $R$  drop was found to be shifted toward lower temperatures as the measuring current density was increased. Possible high-temperature percolative superconductivity with a maximum onset temperature  $T_{c0} \sim 35$  K has, therefore, been proposed (1). Later measurements showed that a magnetic field suppresses the resistance drop (2) and that a diamagnetic signal (2, 11, 12) accompanies the resistance drop associated with a superconducting transition in the 30 K range. Hydrostatic pressure was found (2) to raise  $T_{c0}$ , at an unprecedented rate, to a value of 40.2 K. It was also suggested (2) that a  $T_{c0}$  substantially above 40.2 K may be achievable by the application of pressure together with improvement in the sample conditions. In this report we describe the enhancement of  $T_{c0}$  to above 52 K based on these improvements.

Our earlier studies (2) showed that the increase of the  $\text{K}_2\text{NiF}_4$  phase in the LBCO samples improves the resistance characteristics and raises  $T_{c0}$ . We therefore decided to examine compounds with nominal composition  $(\text{La}_{0.9}\text{Ba}_{0.1})_2\text{CuO}_{4-y}$ , where  $y$  is undetermined. They were prepared by a solid-state reaction (2, 13). The mixture of  $\text{La}_2\text{O}_3$ ,  $\text{CuO}$ , and  $\text{BaCO}_3$  was first heated in air at  $900^\circ\text{C}$  for 4 hours, then was pulverized and heated again in air at  $900^\circ\text{C}$  for 8 hours. The mixture was then pressed into pellets 4.7 mm in diameter for sintering at  $925^\circ\text{C}$  in air for 26 hours. The pellets were finally heated in a reduced  $\text{O}_2$  atmosphere (2000  $\mu\text{m}$  pressure) at  $400^\circ\text{C}$  for 5 hours and then  $900^\circ\text{C}$  for 5 hours. Tests showed that best results were obtained only after the last heat treatment. Samples of dimensions approximately 1 mm by 1 mm by 3 mm were cut from the pellets for measurements. Platinum leads were attached to the samples with gold paste or indium contacts. The standard four-probe technique was used for the measurement of  $R$ . An inductance bridge was used

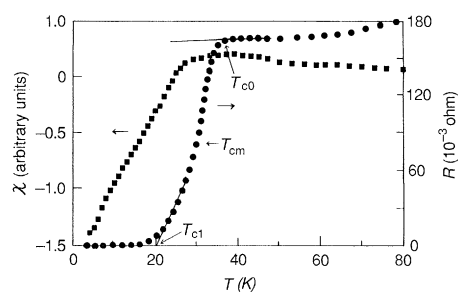


**Fig. 1.** Plot of  $R$  and  $\chi$  as a function of  $T$  at ambient pressure.  $T_{c0}$ , the temperature of superconductivity onset, is defined as the point of deviation from linearity, as shown by the arrow.  $T_{cm}$  is the midpoint temperature at which  $R$  drops to 50% of  $R(T_{c0})$ .  $T_{c1}$  is the intercept of the  $R$  tail with the  $T$  axis.

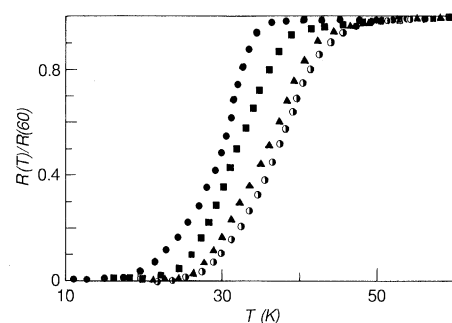


**Fig. 2.** Plot of  $R$  (normalized to its value at 60 K) at different pressures: ●, 0 kbar; ■, 5.7 kbar; ▲, 10.5 kbar; ○, 16.8 kbar.

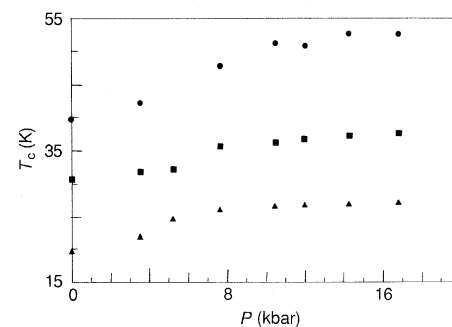


**Fig. 3.** Plot of  $T_c$  as a function of  $P$ : ●,  $T_{c0}$ ; ■,  $T_{cm}$ ; ▲,  $T_{c1}$ .

for the determination of  $\chi$ , the a-c magnetic susceptibility. The temperature was measured with a (iron + 0.07 atomic percent gold)-chromel thermocouple, chromel-alumel thermocouple, or a carbon-glass thermometer in various temperature ranges. The thermometers were calibrated against the (iron + 0.07 atomic percent gold)-chromel thermocouple scale above 4 K, and against the chromel-alumel thermocouple scale above 77 K. Below 23 K, they were calibrated against different standard superconductors. The temperature uncertainty between 25 and 60 K was estimated at  $\pm 0.2$  K. A beryllium-copper high-pressure clamp (14) was used to generate the hydrostatic pressure in a fluid pressure medium. The pres-

sure was measured by a superconducting lead manometer situated next to the samples.

Samples prepared as described above exhibit x-ray powder-diffraction patterns characteristic of the single  $\text{K}_2\text{NiF}_4$  phase within  $\sim 5\%$ . We found that for some sample preparation conditions  $\text{La}_{1-x}\text{Ba}_x\text{CuO}_{3-y}$  can be converted to  $(\text{La}_{1-x}\text{Ba}_x)_2\text{CuO}_{4-y}$  and  $\text{CuO}$ . The electrical properties depend on both the samples and their preparation conditions, as previously suggested (1, 2) but detailed correlations have yet to be determined. The  $R(T)$  of our samples at ambient pressure decreases monotonically with decreasing temperature but at a reduced rate below 60 K. A large  $R$  drop occurs at  $\sim 39$  K, indicative of the onset of a superconducting transition, and  $R$  becomes zero at  $T_{c1} \sim 20$  K as shown in Fig. 1. Preliminary a-c susceptibility measurements showed diamagnetic shifts starting at a temperature of  $\sim 32$  K and reaching a maximum of 10% of the signal of a superconducting lead sample of a similar size. Under hydrostatic pressure the superconducting transition is broadened, but with an overall shift toward higher temperatures as shown in Fig. 2.  $T_{c0}$  has been raised from 39 to 52.5 K and  $T_{c1}$  from 20 to 25 K by a pressure of 12 kbar as displayed in Fig. 3. The rate of increase of  $T_{c0}$  and  $T_{c1}$  is significantly reduced above 12 kbar. The pressure effect on the midpoint temperature  $T_{cm}$  (that is, the temperature where  $R$  has dropped by 50% of  $R$  at  $T_{c0}$ ) is also given in Fig. 3.  $T_{cm}$  increases from 31 to 36 K when placed under pressure. The decrease in the rate of  $T_{c0}$  enhancement above  $\sim 12$  kbar is accompanied by an overall  $R$  increase above  $T_{c0}$ , indicating the possible onset of physical or chemical instabilities. Serious deterioration of samples was also observed upon removal of pressure, as evidenced by the dramatic increase in  $R$  and semiconducting behavior at low temperatures preceded by an  $R$  drop starting at  $T_{c0}$ . The exact causes and remedy for the pressure-induced sample deterioration above  $\sim 12$  kbar are currently under investigation.

The  $\text{K}_2\text{NiF}_4$  layered structure has been proposed (1, 12) to be responsible for the high-temperature superconductivity in LBCO. However, the small diamagnetic signal ( $< 30\%$ ) (2, 11, 12), in contrast to the presence of up to 100% (within a resolution of 5%)  $\text{K}_2\text{NiF}_4$  phase in the samples, raises (2) a question about the exact location of the superconductivity in LBCO. It has been proposed (2) that the superconductivity in LBCO may be associated with an inhomogeneous  $\text{K}_2\text{NiF}_4$  phase, another as yet unidentified phase, or with interfaces between different phases or within an inhomogeneous phase. The current experimental results

cannot rule out unequivocally any of the above possibilities. The large pressure-induced increase of  $T_{c0}$  cannot be understood in terms of current theories. It is consistent, however, with the conjectures (2) of interfacial superconductivity (arising from mixed phases, or interfaces between layers, or concentration fluctuations even within the  $K_2NiF_4$  phase) and noninterfacial superconductivity due to a strong electron-pairing interaction resulting from the mixed valence state in LBCO. A  $d$ - $f$  mixing due to  $f$ -electrons in lanthanum slightly above the Fermi level can lead to a high electron density of states and thus a high  $T_c$ . This mixing is also sensitive to pressure. This possibility can be tested in future specific heat measurements. Finally, it should be pointed out that the  $T_{c0}$  observed by us

exceeds the limit previously predicted by theory (15) based on the conventional electron-phonon interaction.

#### REFERENCES AND NOTES

1. J. G. Bednorz and K. A. Müller, *Z. Phys. B* **64**, 189 (1986).
2. C. W. Chu *et al.*, *Phys. Rev. Lett.*, in press.
3. J. R. Gavaler, *Appl. Phys. Lett.* **23**, 480 (1973); L. R. Testardi, J. H. Wernick, W. A. Royer, *Solid State Commun.* **15**, 1 (1974).
4. For a review, see P. A. Lee *et al.*, *Comments Condensed Matter Phys.*, **12**, 99 (1986); Z. Fisk *et al.*, *Nature (London)* **320**, 124 (1986).
5. C. W. Chu and M. K. Wu, in *High Pressure in Science and Technology*, C. Homan, R. K. MacCrone, E. Whalley, Eds. (North-Holland, New York, 1983), vol. 1, p. 3.
6. SrTiO<sub>3-x</sub>: J. F. Scholey, W. R. Hosler, M. L. Cohen, *Phys. Rev. Lett.* **12**, 474 (1964); Na<sub>2</sub>WO<sub>3</sub>: H. R. Shank, *Solid State Commun.* **15**, 753 (1974); Li<sub>1-x</sub>Ti<sub>2-x</sub>O<sub>4</sub>: D. C. Johnston, H. Prakash, W. H. Zachariosen, R. Viswanathan, *Mater. Res. Bull.* **8**, 777 (1973); BaPb<sub>1-x</sub>Bi<sub>x</sub>O<sub>3</sub>: A. W. Sleight, J. L.

- Gillson, F. E. Bielsch, *Solid State Commun.* **17**, 27 (1975).
7. C. W. Chu, S. Huang, A. W. Sleight, *Solid State Commun.* **18**, 977 (1976).
8. See, for example, L. R. Testardi, in *Physical Acoustics*, W. P. Mason and R. N. Thurston, Eds. (Academic Press, New York, 1973), vol. 1, p. 193.
9. See, for example, J. Bardeen, in *Superconductivity in d- and f-Band Metals*, D. Douglas, Ed. (Plenum, New York, 1973), p. 1; T. H. Geballe and C. W. Chu, *Comments Solid State Phys.* **9**, 115 (1979).
10. See, for example, B. K. Chakraverty, *J. Phys. C* **42**, 1351 (1981).
11. J. G. Bednorz, M. Takashige, K. A. Müller, *Eur. Phys. Lett.*, in press.
12. S. Uchida, H. Takagi, K. Kitazawa, S. Tanaka, *Jpn. J. Appl. Phys.*, in press; H. Takagi, S. Uchida, K. Kitazawa, S. Tanaka, *ibid.*, in press.
13. C. Michel and B. Raveau, *Rev. Chim. Miner.* **21**, 407 (1984).
14. C. W. Chu, T. F. Smith, W. E. Gardner, *Phys. Rev. Lett.* **20**, 198 (1968).
15. W. McMillan, *Phys. Rev.* **167**, 331 (1968).
16. This work was supported in part by NSF grant DMR-8204173, NASA grant NAGW-977, and the Energy Laboratory of the University of Houston. 30 December 1986; accepted 9 January 1987

## Evaluation of Intrinsic Binding Energy from a Hydrogen Bonding Group in an Enzyme Inhibitor

PAUL A. BARTLETT\* AND CHARLES K. MARLOWE

This and two accompanying reports describe the intrinsic binding energy derived from a single hydrogen bond between an inhibitor and an enzyme. The results were obtained by comparing matched pairs of inhibitors of the zinc endopeptidase thermolysin that bind to the enzyme in an essentially identical manner but differ in the presence or absence of a specific hydrogen bond. This report describes five phosphorus-containing analogs of the peptides carbobenzoxy-Gly-Leu-X, in which the Gly-Leu peptide linkage is replaced with a phosphonate ester (-PO<sub>2</sub><sup>-</sup>-O-). Values for the inhibition constants of these inhibitors show a direct relation with those of the corresponding phosphoramidate analogs (-PO<sub>2</sub><sup>-</sup>-NH- in place of the Gly-Leu peptide moiety), which have been characterized previously as transition state analogs. However, each phosphonate ester is bound about 840 times more weakly than the analogous phosphoramidate, reflecting the loss of 4.0 ± 0.1 kilocalories per mole in binding energy. From these results and the crystallographic analysis in the next report, it can be inferred that the value of 4.0 kilocalories per mole represents the intrinsic binding energy arising from a highly specific hydrogen bonding interaction.

**A** GOAL YET TO BE ATTAINED IN THE study of any enzyme mechanism is a full understanding of the relations among active site structure, substrate binding, and the dynamics of catalysis (1). While we have a qualitative understanding of the interactions between substrates and enzyme active sites, quantitative understanding of the roles played by separate substructural elements is clouded by the difficulty in distinguishing effects due to solvation and, in particular, entropy. Jencks has pointed out that the incremental change in Gibbs (G) free energy of binding due to the addition of a group X to a reference molecule A provides a measure of the "intrinsic binding energy" due to X (Eq. 1) (2). This value is free from entropic complications if A and

A-X do not undergo differences in strain or in rotational and translational entropy loss on binding to the enzyme (2). However, these qualifications are not easily met, especially in view of the fact that, as an appendage to A, the X-moiety seldom represents an insignificant structural perturbation. Moreover, the attribution of observed intrinsic binding energies to a specific interaction is risky in the absence of corroborating structural information.

$$(\Delta G_X^i = \Delta G_{A-X}^0 - \Delta G_A^0) \quad (1)$$

We previously reported that phosphoramidate peptide analogs 1, X = NH<sub>2</sub> or amino acid (ZG<sup>P</sup>LX; see Table 1), are potent inhibitors of the zinc endopeptidase thermolysin, and that their free energies of

interaction with the enzyme, reflected in the inhibition constants  $K_i$ , show a strong correlation with the (hypothetical) binding energies of the transition states for hydrolysis of the corresponding amide substrates, reflected in the second order rate constants for enzymatic turnover ( $K_m/k_{cat}$ ) (3). From this correlation we concluded that the phosphoramidates mimic the transition state configurations of the enzyme-substrate complexes (4). We now report our findings with a series of phosphonate esters 2 [ZG<sup>P</sup>(O)LX], which differ from the amidates in replacement of the NH linkage between phosphorus and the leucine moiety with an oxygen atom (5). The structural consequences of this substitution are minimal; however, the effect that it has on the magnitude of  $K_i$  is significant (Fig. 1 and Table 1).

Replacement of the phosphoramidate NH with phosphonate O reduces the binding energy of each inhibitor by a factor of 840, almost uniformly across the two orders of magnitude in absolute binding affinity within each series. The constancy of this increment reflects an identical correlation between structural variation and binding energy within each series, and therefore suggests that the phosphoramidate and phosphonate inhibitors bind to the enzyme active site in a similar manner, and, aside from those due to the NH group itself, with similar interactions with the protein. The difference in  $K_i$  values between the phosphoramidates and phosphonates represents

Department of Chemistry, University of California, Berkeley, CA 94720.

\*To whom correspondence should be addressed.